

# Simulation and Hardware Implementation of High Efficiency Single Input Multiple Output (SIMO) DC-DC Converter using Fuzzy Logic Control

R. Meenakshi

Assistant Professor, Department of Computer Science, Nazareth college of arts and science, Chennai.

**Abstract :** This paper describes simulation and hardware implementation of single-input multiple-output (SIMO) dc-dc converter. The proposed converter can boost the low voltage input and give multiple outputs. As multiple outputs are obtained in this converter, it can be used to power a multilevel inverter which needs more than single source. This paper presents how a single switch can be used and utilized in a efficient manner with the properties of voltage clamping and soft switching, and the corresponding device specifications are adequately designed. As a result, the objectives of high-efficiency power conversion, high step up ratio, and various output voltages with different levels can be obtained. The Fuzzy Logic control scheme is used to control the gating sequence of power switch.

**Keywords:** Single input multiple output converter, Fuzzy logic Controller, PWM, Mosfet Switch.

## 1. Introduction

The main aim of this study is to develop a single input multiple output converter with increased conversion efficiency, high step up ratio, saving the manufacturing cost. In the single input multiple output system is implemented by using Fuzzy Logic control. In order to protect the natural environment on the earth, the development of clean energy without pollution has the major representative role in the last decade. By dealing with the issue of global warming, clean energies, such as fuel cell (FC), photovoltaic, and wind energy, etc., have been rapidly promoted. Due to the electric characteristics of clean energy, the generated power is critically [1] affected by the climate or has slow transient responses, and the output voltage is easily influenced by load variations. For example, an FC-generation system is one of the most efficient and effective solutions to the environmental pollution problem. [2]

In addition to the FC stack itself, some other auxiliary components, such as the balance of plant (BOP) including an electronic control board, an air compressor, and a cooling fan, are required for the normal work of an FC generation system. [4]

In other words, the generated power of the FC stack also should satisfy the power demand for the BOP. Thus, various voltage levels should be required in the power converter of an FC generation system.

In general, various SIMO dc-dc converters with different voltage gains are combined to satisfy the requirement of various voltage levels, so that its system control is more complicated and the corresponding cost is more expensive. [10]

## 2. Existing System

The SISO (single input and single output) system proposed a single input. This single-input and single-output (SISO) system has a simple single variable control system with one input and one output. The controller exhibits output voltage regulation characteristic that is robust against load variations and reference voltage changes. [11]

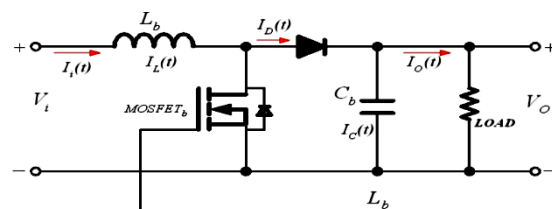


Figure 2.1 Single input single output system

## 2.2 Modes Of Operation:

### Mode 1 ( $0 < t \leq t_{on}$ ),

Mode 1 starts, when switch S (MOSFET) switched on at  $t = 0$  until  $t = t_{on}$ . By assuming that the serial resistance value DC voltage source is relatively low, there will be an inductor current transient  $i_L(t)$  larger than zero and increase linearly at the beginning of transient. Inductor voltage is  $V_L = V_i$ .

### Mode 2 ( $t_{on} < t \leq T_s$ ),

Mode 2 starts, when switch S (MOSFET) switched off at  $t = t_{on}$  until  $t = T_s$ . Inductor voltage,  $V_L$  in this period is  $V_i - V_o$ . In this case  $V_i < V_o$ , it means in Mode 2,  $V_L$  is in opposite direction to  $V_L$  in Mode 1.

## 2.3 Existing System Disadvantages:

In general, various single-input single-output dc–dc converters with different voltage gains are combined to satisfy the requirement of various voltage levels, so that its system control is more complicated and the corresponding cost is more expensive.[11]

### 3. Proposed System

The proposed converter can boost the voltage of a low-voltage input power source to a controllable high-voltage dc bus and middle-voltage output terminals. The newly designed multi output converter with a coupled inductor uses only one power switch with the properties of voltage clamping and soft switching, and the corresponding device specifications are adequately designed to boost the voltage levels. As a result, the objectives of high-efficiency power conversion, high step up ratio, and various output voltages with different levels can be obtained. The basic requirements of this converter is small size and high efficiency. High switching frequency is necessary for achievement of small size. If the switching frequency is increased then the switching loss will increase. It decreases the efficiency of the power supplies. To solve this problem, some kinds of soft switching techniques need to be used to operate under high switching frequency.

The techniques of soft switching and voltage clamping are adopted switching and conduction losses via the utilization of a low-voltage-rated power switch with a small  $RDS(on)$ . The slow rate of the current change in the coupled inductor can be restricted by the leakage inductor, the current transition time enables the power switch to turn ON with the ZCS property easily, and the effect of the leakage inductor can alleviate the losses caused by the reverse-recovery current. Additionally, the problems of the stray inductance energy and reverse-recovery currents within diodes in the conventional boost converter also can be solved, so that the high-efficiency power conversion can be achieved. The voltages of middle-voltage output terminals can be appropriately adjusted by the design of auxiliary inductors; the output voltage of the high-voltage dc bus can be stably controlled by a Fuzzy Logic control.

#### 3.1 Proposed System Advantages:

This topology adopts only one power switch to achieve the objective of high-efficiency SIMO power conversion. The voltage gain can be substantially increased by using a coupled inductor. The copper loss in the magnetic core can be greatly reduced. The developing cost is Low and the size is reduced. This system provides high efficiency comparing with the existing system.[12]

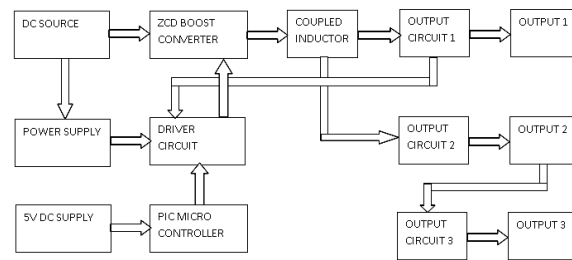


Figure 3.1.1 Block diagram of single input multiple output system.

Proposed Single Input Multiple Output dc - dc converter, the DC Source block consists of the dc input power source and a capacitor. The value of input is in the range of 12V. Switch Integrated with Coupled Inductor block consisting of a coupled inductor, a MOSFET switch and a diode. The coupled inductor primary has a series connected leakage inductor and a parallel connected magnetizing inductor. Output Voltage 1 Circuit consists of an auxiliary inductor, a diode and a filter capacitor. The value of output voltage 1 is 28V. Output Voltage 2 Circuit consists of a capacitor connected in series with the coupled inductor secondary and a diode connected in parallel with the above combination. In addition, the series connected diode and a filter capacitor is used. The value of output voltage 2 is 200V. Output Voltage 3 circuit consists of two MOSFET switches, two diodes and two capacitors. The value of output voltage 3 is - 200V.[12]

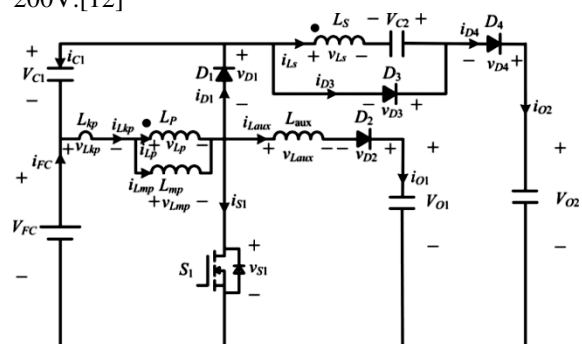


Figure 3.1.2 Proposed single input multiple output system

The system configuration of the proposed SIMO converter topology to generate three different voltage levels from a single-input power source. This SIMO converter contains five parts ,

- An input side circuit (ISC)
- A clamped circuit
- A coupled inductor secondary circuit
- Output voltage 1 circuit
- Output voltage 2circuit

VFc (ifc) and V01(i01) denote the voltages (currents) of the input power source and the output load at the input side voltage circuit and the output

voltage 1 circuit, respectively. VO2 and iO2 are the output voltage and current in the HVSC. CFC, CO1 , and CO2 are the filter capacitors. C1 and C2 are the clamped and middle-voltage capacitors in the clamped and middle-voltage circuits. LP and LS represent individual inductors in the primary and secondary sides of the coupled inductor, where the primary side is connected to the input power source. Laux is the auxiliary circuit inductor. [11]

The main switch is expressed as S1; the equivalent load in the auxiliary circuit is represented as RO1 , and the output load is represented as RO 2 in the HVSC. The coupled inductor can be modeled as an ideal transformer including the magnetizing inductor Lmp and the leakage inductor Lkp. The turn's ratio N and coupling coefficient k of this ideal transformer are defined in equations 1 & 2 as,

$$N = N2/N1$$

$$k = Lmp / (Lkp + Lmp) = Lmp/LP$$

N1 and N2 are the winding turns in the primary and secondary sides of the coupled inductor . Because the voltage gain is less sensitive to the coupling coefficient and the clamped capacitor C1 is appropriately selected to completely absorb the leakage inductor energy, the coupling coefficient set at unity to obtain Lmp= LP. Some assumptions are made to simplify the converter analyses:

- 1) Main switch is assumed to be an ideal switching element
- 2) The conduction voltage drops of the switch and diodes are neglected

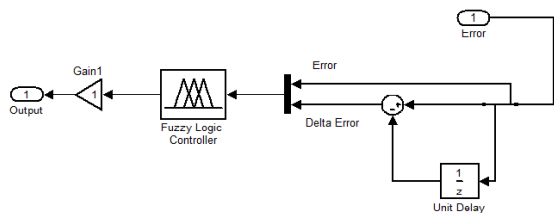


Figure 3.1.3 control scheme by Fuzzy logic control

#### 4. Modes of Operation

##### Mode 1 (t0 –t1):

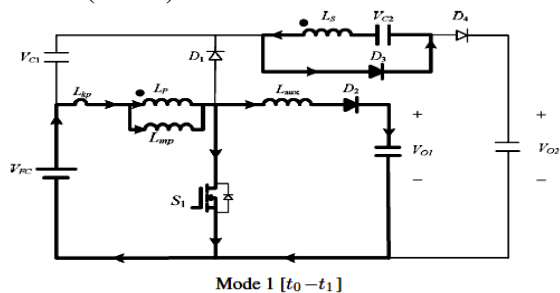


Figure 4.1 Mode1 operation of SIMO

The main switch S1 was turned ON, and the diode D4 turned OFF. Because the polarity of the

windings of the coupled inductor is positive, the diode D3 turns ON. The secondary current iLS reverses and charges to the middle voltage capacitor C2 . When the auxiliary inductor Laux releases its stored energy completely, and the diode D2 turns OFF, this mode ends. [13]

##### Mode 2 (t1 –t2) :

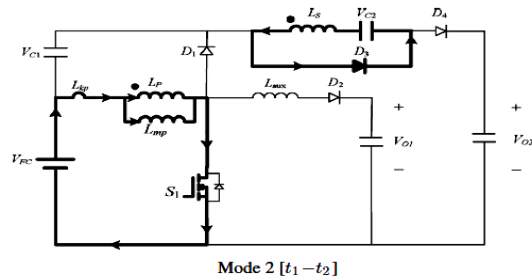


Figure 4.2 Mode 2 operation of SIMO

At time t = t1 , the main switch S1 is persistently turned ON. Because the primary inductor LP is charged by the input power source, the magnetizing current iLmp increases gradually in an approximately linear way. At the same time, the secondary voltage vLS charges the middle-voltage capacitor C2 through the diode D3 . Although the voltage vLmp is equal to the input voltage VFC at modes 1 and 2, the leakage current of the coupled inductor (diLkp /dt) at these modes are different due to the path of the auxiliary circuit. Because the auxiliary inductor Laux releases its stored energy completely, and the diode D2 turns OFF at the end of mode 1, it results in the reduction of diLkp /dt at mode 2.

##### Mode 3 (t2 –t3) :

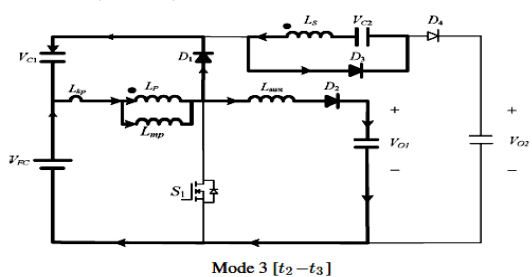
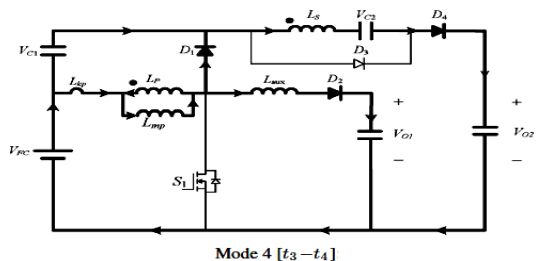


Figure 4.3 Mode 3 operation of SIMO

At time t = t2 , the main switch S1 is turned OFF. When the leakage energy still released from the secondary side of the coupled inductor, the diode D3 persistently conducts and releases the leakage energy to the middle-voltage capacitor C2 . When the voltage across the main switch vS 1 is higher than the voltage across the clamped capacitor VC 1 , then the diode D1 conducts and to transmit the energy of the primary-side leakage inductor Lkp into the clamped capacitor C1 . At the same time, partial energy of the primary-side leakage inductor Lkp is transmitted to the auxiliary inductor Laux, and the

diode D2 conducts. Thus, the current  $i_{L_{aux}}$  passes through the diode D2 to give power for the output load in the auxiliary circuit. When the secondary side of the coupled inductor releases its leakage energy completely, and the diode D3 turns OFF, this mode ends.

**Mode 4 ( $t_3 - t_4$ ) :**

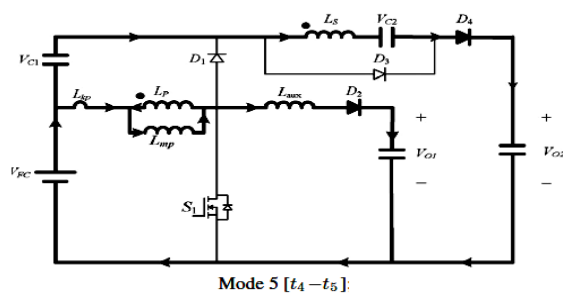


**Figure 4.4 Mode 4 operation of SIMO**

At time  $t = t_3$ , the main switch S1 is turned OFF. When the leakage energy has released from the primary side of the coupled inductor, the secondary current  $i_L$  is induced in reverse from the energy of the magnetizing inductor  $L_{mp}$  through the ideal transformer, and flows through the diode D4 to the HVSC. At the same time, partial energy of the primary side leakage inductor  $L_{kp}$  is still persistently transmitted to

the auxiliary inductor  $L_{aux}$ , and the diode D2 keeps to conduct. Moreover, the current  $i_{L_{aux}}$  passes through the diode D2 to supply the power for the output load in the auxiliary circuit.

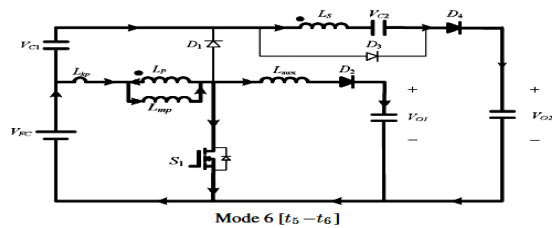
**Mode 5 ( $t_4 - t_5$ ) :**



**Mode 5 ( $t_4$ )**  
**Figure 4.5 Mode 5 operation of SIMO**

At time  $t = t_4$ , the main switch S1 is turned OFF, and the clamped diode D1 turns OFF because the primary leakage current  $i_{L_{kp}}$  equals to the auxiliary inductor current  $i_{L_{aux}}$ . In this mode, the input power source, the primary winding of the coupled inductor  $Tr$ , and the auxiliary inductor  $L_{aux}$  connect in series to supply the power for the output load in the auxiliary circuit through the diode D2. Since the clamped diode D1 can be selected as a low-voltage Schottky diode, it will be cut off promptly without a reverse-recovery current. Moreover, the rising rate of the primary current  $i_{L_{kp}}$  is limited by primary-side

leakage inductor  $L_{kp}$ . Thus, one cannot derive any currents from the paths of the HVSC, the middle-voltage circuit, the auxiliary circuit, and the clamped circuit.



**Mode 6 ( $t_5 - t_6$ ) :**

**Figure 4.6 Mode 6 operation of SIMO**

At time  $t=t_5$ , this mode begins when the main switch S1 is triggered. The auxiliary inductor current  $i_{L_{aux}}$  needs time to decay to zero, the diode D2 persistently conducts. In this mode, the input power source, the clamped capacitor C1, the secondary winding of the coupled inductor  $Tr$ , and the middle-voltage capacitor C2 still connect in series to release the energy into the HVSC through the diode D4.

## 5. Simulink Model and Results

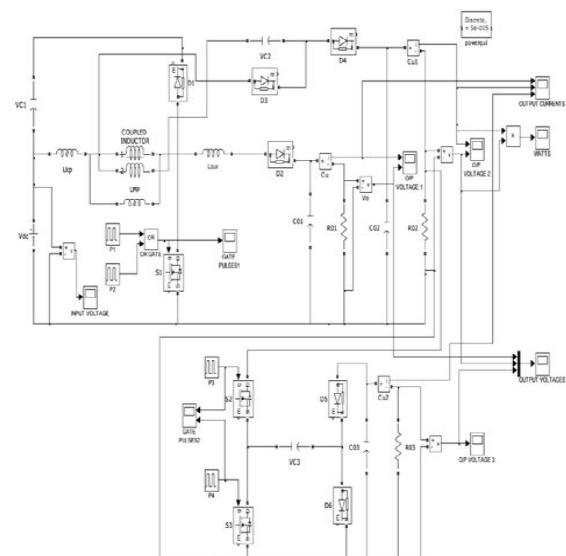


**Fig 5.1 Simulink Model of SIMO converter.**

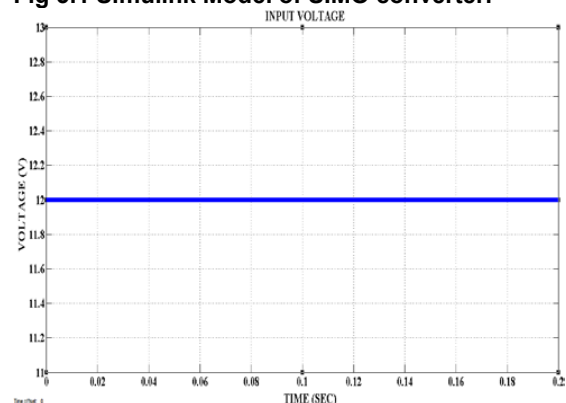


Figure 5.2 Input Voltage

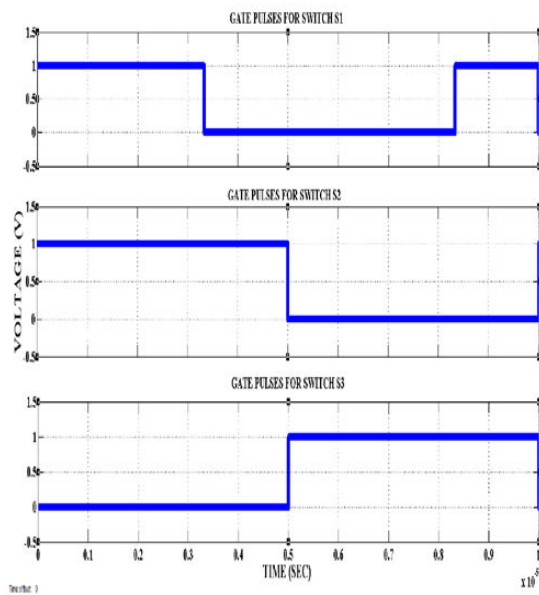


Figure 5.3 Gate pulses of switch  $S_1, S_2$  &  $S_3$

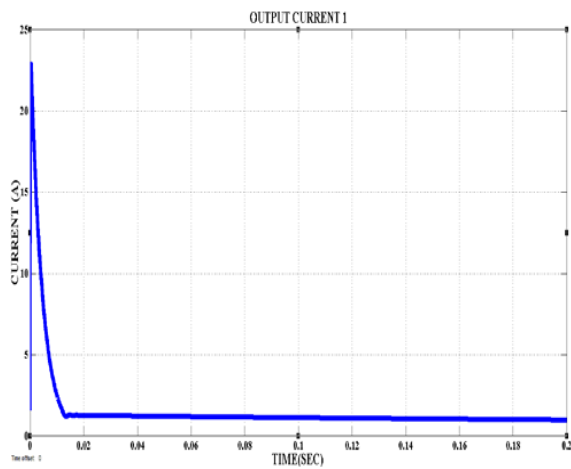


Figure 5.4 Output current at terminal 1 of the proposed circuit

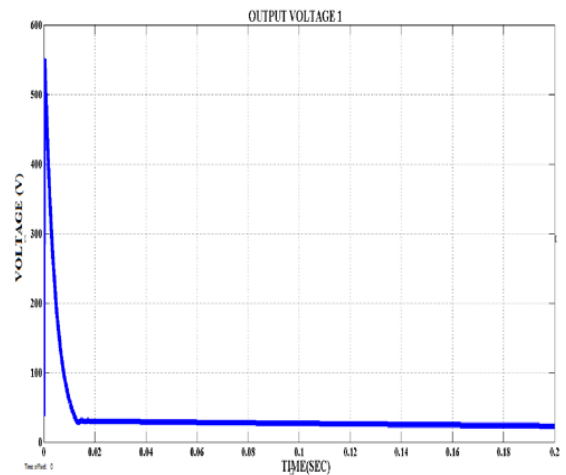


Figure 5.5 Output voltage at terminal 1 of the proposed circuit

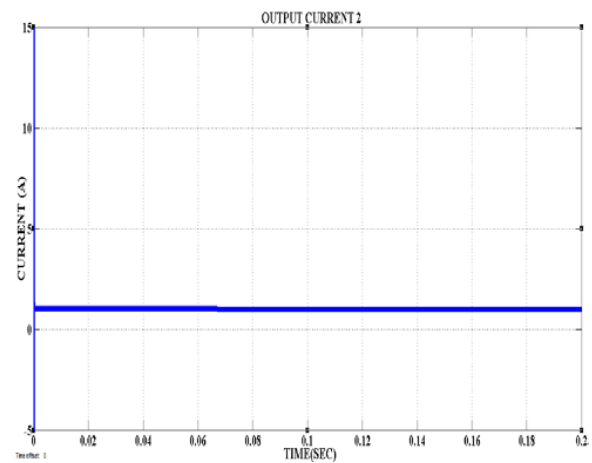


Figure 5.6 Output current at terminal 2 of the proposed circuit

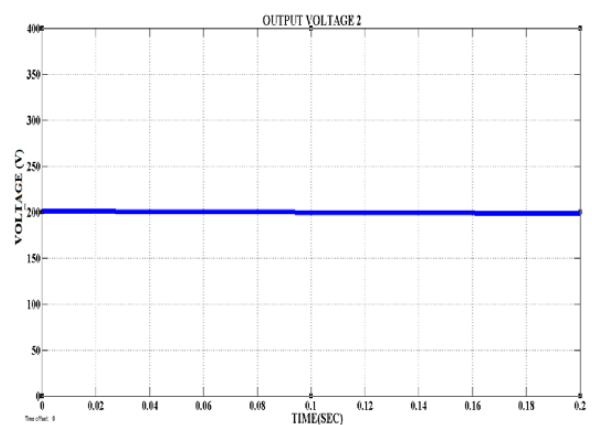


Figure 5.7 Output voltage at terminal 2 of the proposed circuit



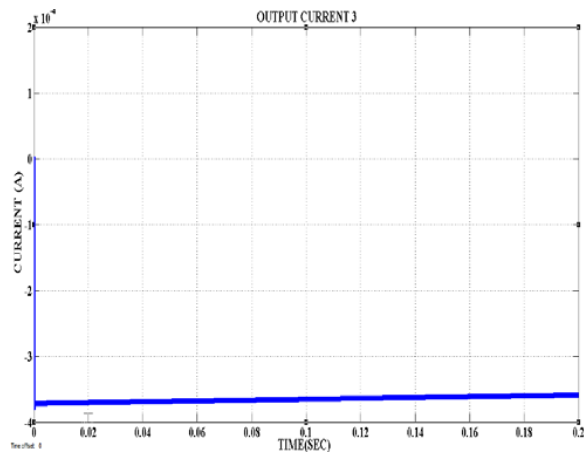


Figure 5.8 Output current at terminal 3 of the proposed circuit

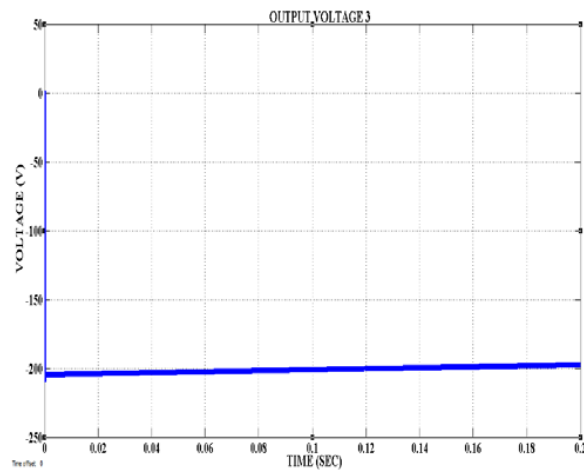


Figure 5.9 Output voltage at terminal 3 of the proposed circuit

## 6. Hardware Implementation

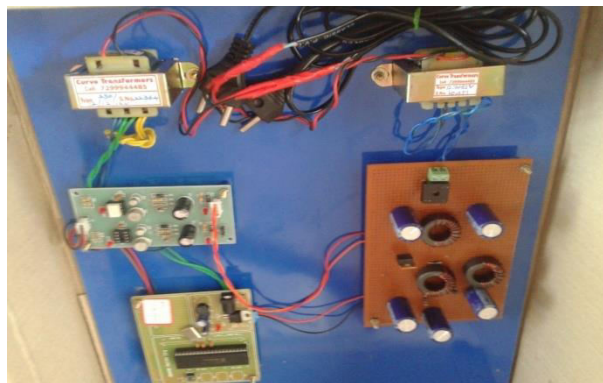


Figure 6.1 Hardware implementation of SIMO

## 7. Conclusion

This proposed system has presented high - efficiency dc - dc converter, and this coupled - inductor - based converter was applied well to a single - input power source having two output terminals of an auxiliary battery module and a high - voltage dc bus. The results of SIMO converter is the maximum efficiency was measured to be exceed 95%, and the average conversion efficiency was measured over 91%. The proposed SIMO converter is suitable for the application such as one common ground, is preferred in most applications. The major scientific contributions of the SIMO converter are recited as follows:

- This topology has only one power switch to achieve the objective of SIMO power conversion.
- The voltage gain is substantially increased by using a coupled inductor
- The stray energy is recycled by a clamped capacitor into the auxiliary battery module or high - voltage dc bus to ensure the property of voltage clamping.
- An auxiliary inductor is providing the charge power to the auxiliary battery module and assisting the turned ON under the conditions of ZCS.
- The switch voltage stress is not on the input voltage so that it is more suitable for a dc conversion mechanism with different input voltage levels.
- The copper loss in the magnetic core can be greatly reduced, due to copper film with lower turns.

## 8. References

- [1] A. Kirubakaran, S. Jain, and R. K. Nema, "DSP-controlled power electronic interface for fuel-cell-based distributed generation," IEEE Trans. Power Electron., vol. 26, no. 12, pp. 3853–3864, Dec. 2011.
- [2] B. Liu, S. Duan, and T. Cai, "Photovoltaic dc-building-module-based BIPV system-concept and design considerations," IEEE Trans. Power Electron., vol. 26, no. 5, pp. 1418–1429, May 2011.
- [3] M. Singh and A. Chandra, "Application of adaptive network-based fuzzy interference system for sensorless control of PMSG-based wind turbine with nonlinear-load-compensation capabilities," IEEE Trans. Power Electron., vol. 26, no. 1, pp. 165–175, Jan. 2011.
- [4] C. T. Pan, M. C. Cheng, and C.M. Lai, "A novel integrated dc/ac converter with high voltage gain capability for distributed energy resource systems," IEEE Trans. Power Electron., vol. 27, no. 5, pp. 2385–2395, May 2012.

[5] S. D. Gamini Jayasinghe, D. Mahinda Vilathgamuwa, and U. K. Madawala, "Diode-clamped three-level inverter-based battery/supercapacitor direct integration scheme for renewable energy systems," *IEEE Trans. Power Electron.*, vol. 26, no. 6, pp. 3720–3729, Dec. 2011.

[6] H. Wu, R. Chen, J. Zhang, Y. Xing, H. Hu, and H. Ge, "A family of threeport half-bridge converters for a stand-alone renewable power system," *IEEE Trans. Power Electron.*, vol. 26, no. 9, pp. 2697–2706, Sep. 2012.

[7] M. W. Ellis, M. R. Von Spakovsky, and D. J. Nelson, "Fuel cell systems: Efficient, flexible energy conversion for the 21<sup>st</sup> century," *Proc. IEEE*, vol. 89, no. 12, pp. 1808–1818, Dec. 2001.

[8] T. Kim, O. Vodyakho, and J. Yang, "Fuel cell hybrid electronic scooter," *IEEE Ind. Appl. Mag.*, vol. 17, no. 2, pp. 25–31, Mar./Apr. 2011.

[9] F. Gao, B. Blunier, M. G. Simões, and A. Miraoui, "PEM fuel cell stack modeling for real-time emulation in hardware-in-the-loop application," *IEEE Trans. Energy Convers.*, vol. 26, no. 1, pp. 184–194, Mar. 2011.

[10] P. Patra, A. Patra, and N. Misra, "A single-inductor multiple-output switcher with simultaneous buck, boost and inverted outputs," *IEEE Trans. Power Electron.*, vol. 27, no. 4, pp. 1936–1951, Apr. 2012.

[11] A. Nami, F. Zare, A. Ghosh, and F. Blaabjerg, "Multiple-output DC–DC converters based on diode-clamped converters configuration: Topology and control strategy," *IET Power Electron.*, vol. 3, no. 2, pp. 197–208, 2010.

[12] Y. Chen, Y. Kang, S. Nie, and X. Pei, "The multiple-output DC–DC converter with shared ZCS lagging leg," *IEEE Trans. Power Electron.*, vol. 26, no. 8, pp. 2278–2294, Aug. 2011.